

**Ultrahigh Capacity 2D Anode Materials for Lithium/Sodium-Ion Batteries:**

**Entirely Planar B<sub>7</sub>P<sub>2</sub> monolayer with Proper Pore Size and Distribution**

Changyan Zhu,<sup>a</sup> Shiru Lin,<sup>b</sup> Min Zhang,<sup>\*,a</sup> Quan Li,<sup>c</sup>

Zhongmin Su,<sup>a,d</sup> Zhongfang Chen<sup>\*,b</sup>

<sup>a</sup> Institute of Functional Material Chemistry, Faculty of Chemistry & National & Local United Engineering Laboratory for Power Battery, Northeast Normal University, Changchun 130024, China

<sup>b</sup> Department of Chemistry, Institute for Functional Nanomaterials, University of Puerto Rico Rio, Rio Piedras Campus, San Juan, PR 00931, USA

<sup>c</sup> State Key Laboratory of Superhard Materials, Key Laboratory of Automobile Materials of MOE, Department of Materials Science, and Innovation Center for Computational Physics Method and Software, Jilin University, Changchun 130012, China

<sup>d</sup> School of Chemistry and Environmental Engineering, Changchun University of Science and Technology, Changchun 130024, China

## **Maximum Na storage capacity of the entirely planar and porous $\beta_{12}$ -borophene**

In the literature, the maximum Na storage capacity of the entirely planar and porous  $\beta_{12}$ -borophene is 1984 mA h g<sup>-1</sup>, corresponding to B<sub>5</sub>Na<sub>4</sub> with single-layer Na atoms.<sup>7</sup> Is it possible to adsorb two-layer Na atoms on the  $\beta_{12}$ -borophene?

To address this question, we re-evaluated the maximum Na storage capacity on the  $\beta_{12}$ -borophene. Four different concentrations, which correspond to the chemical stoichiometries of B<sub>40</sub>Na<sub>16</sub>, B<sub>40</sub>Na<sub>32</sub>, B<sub>40</sub>Na<sub>48</sub> and B<sub>40</sub>Na<sub>64</sub>, respectively, were considered. Fig. S1 presents the most stable structures and the average Na adsorption energies with different Na concentrations. Note that at the highest concentration considered (B<sub>40</sub>Na<sub>64</sub>), the calculated average adsorption energies are -0.18 eV/Na atom, and the Na atoms prefer to being separately adsorbed on the  $\beta_{12}$ -borophene in two layers. Thus, the Na storage on the  $\beta_{12}$ -borophene can reach such a high ratio without suffering the Na clustering problem. The calculated maximum theoretical storage capacity of the entirely planar and porous  $\beta_{12}$ -borophene (corresponding to B<sub>40</sub>Na<sub>64</sub>) is 3968 mA h g<sup>-1</sup>, which is much higher than that on the puckered triangular-borophene (2341 mA h g<sup>-1</sup>).

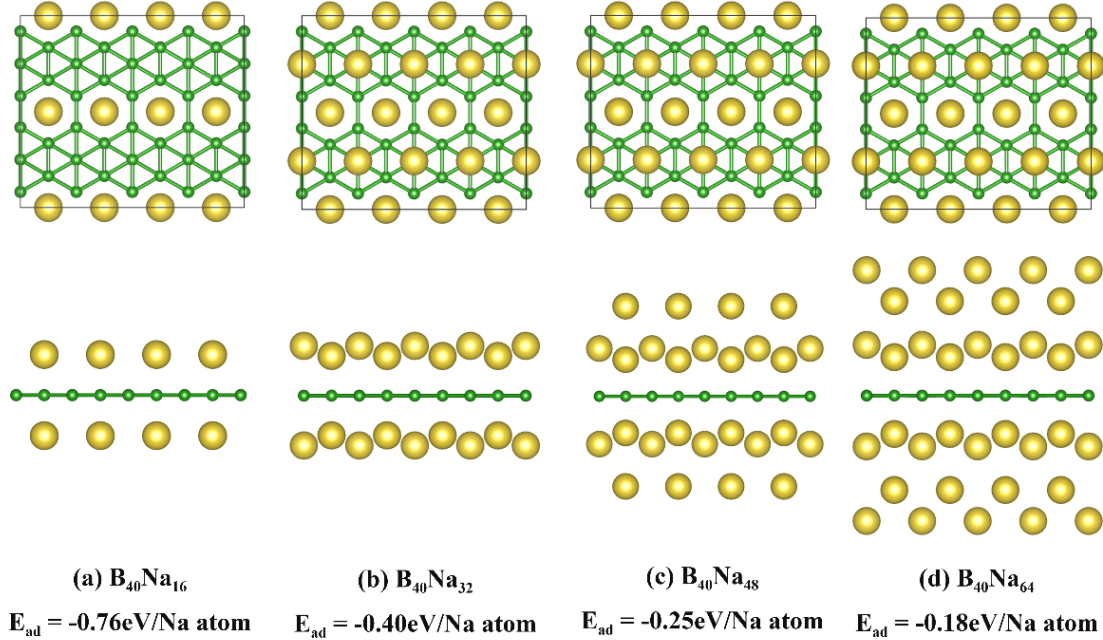


**Fig. S1** The most stable structures and the corresponding average adsorption energy of Na atoms adsorbed on the entirely planar and porous  $\beta_{12}$ -borophene with different sodiation ratios.

### Validation of our computational methods

To test the reliability of the adopted function and pseudopotentials, we compared the lattice parameters of graphene, triangular-borophene,  $\beta_{12}$ -borophene and  $\chi_3$ -borophene at our computational level with those reported in experiments and previous theoretical studies. As summarized in Table S1, clearly our optimized lattice parameters are in agreement with the experimental results, except for the lattice parameter  $b$  of triangular-borophene, which is slightly higher than 5% due to the dihedral angel error in the puckered structure. Note that our optimized lattice parameter  $b$  of triangular-borophene is consistent with previous theoretical results ( $1.613 \text{\AA}^1$  and  $1.614 \text{\AA}^2$ ).

**Table S1.** Lattice parameters  $a$  and  $b$  of graphene, triangular-borophene,  $\beta_{12}$ -borophene and  $\chi_3$ -borophene in experiment and theory, as well as the error.

Lattice parameter(Å)	Experiment	Theoretical (previous)	Theory (this work)	Error(expt.)	Error(theor.)
Graphene- $a(b)$	2.42 <sup>3</sup>	2.464 <sup>4</sup>	2.467	0.285%	0.122%
triangular-borophene- $a$	2.9 <sup>5</sup>	2.861 <sup>2</sup>	2.872	0.966%	0.384%
triangular-borophene- $b$	1.7 <sup>5</sup>	1.614 <sup>2</sup>	1.614	5.059%	0.000%
$\beta_{12}$ -borophene- $a$	3.0 <sup>6</sup>	2.926 <sup>7</sup>	2.928	2.400%	0.068%
$\beta_{12}$ -borophene- $b$	5.0 <sup>6</sup>	5.068 <sup>7</sup>	5.071	1.420%	0.059%
$\chi_3$ -borophene- $a(b)$	4.3 <sup>6</sup>	4.490 <sup>7</sup>	4.450	3.488%	0.891%

**Table S2.** Bader charge and Hirshfeld charge analysis of  $2 \times 2$   $B_7P_2$  supercell adsorbing single Li/Na atom at three different adsorption sites.

Charge( e )	Bader-M	Bader- $B_{28}P_8$	Hirshfeld-M	Hirshfeld- $B_{28}P_8$
$B_{28}P_8$ -Li1	+0.866	-0.866	+0.357	-0.357
$B_{28}P_8$ -Li2	+0.872	-0.872	+0.397	-0.397
$B_{28}P_8$ -Li3	+0.892	-0.892	+0.416	-0.416
$B_{28}P_8$ -Na1	+0.846	-0.846	+0.511	-0.511
$B_{28}P_8$ -Na2	+0.867	-0.867	+0.556	-0.556
$B_{28}P_8$ -Na3	+0.866	-0.866	+0.536	-0.536

**Table S3.** Open-circuit voltage (OCV) of the  $B_7P_2(Li/Na)_n$  ( $n=1-16$ ) for LIBs and SIBs.

OCV (V)	$B_7P_2Li_1$ 1.39	$B_7P_2Li_2$ 1.03	$B_7P_2Li_3$ 1.00	$B_7P_2Li_4$ 1.08
OCV (V)	$B_7P_2Li_5$ 0.98	$B_7P_2Li_6$ 0.78	$B_7P_2Li_7$ 0.67	$B_7P_2Li_8$ 0.61
OCV (V)	$B_7P_2Li_9$ 0.54	$B_7P_2Li_{10}$ 0.51	$B_7P_2Li_{11}$ 0.45	$B_7P_2Li_{12}$ 0.39
OCV (V)	$B_7P_2Li_{13}$ 0.35	$B_7P_2Li_{14}$ 0.33	$B_7P_2Li_{15}$ 0.31	$B_7P_2Li_{16}$ 0.28
OCV (V)	$B_7P_2Na_1$ 1.01	$B_7P_2Na_2$ 0.71	$B_7P_2Na_3$ 0.57	$B_7P_2Na_4$ 0.63
OCV (V)	$B_7P_2Na_5$ 0.64	$B_7P_2Na_6$ 0.55	$B_7P_2Na_7$ 0.50	$B_7P_2Na_8$ 0.46
OCV (V)	$B_7P_2Na_9$ 0.41	$B_7P_2Na_{10}$ 0.39	$B_7P_2Na_{11}$ 0.36	$B_7P_2Na_{12}$ 0.32
OCV (V)	$B_7P_2Na_{13}$ 0.30	$B_7P_2Na_{14}$ 0.30	$B_7P_2Na_{15}$ 0.27	$B_7P_2Na_{16}$ 0.24

**Table S4.** Structural parameters of the optimized B<sub>7</sub>P<sub>2</sub> monolayer.

Phase	Space Group	Lattice Parameters (Å, °)	Coordinates
B <sub>7</sub> P <sub>2</sub>	P6/MMM	$a = 6.11998$ $b = 4.35599$ $c = 30.00000$ $\alpha = \beta = 90.00000$ $\gamma = 120.00000$	B(0.160062566, 0.839937449, 0.500000000) B(0.839937449, 0.160062566, 0.500000000) B(0.160062566, 0.320125133, 0.500000000) B(0.839937449, 0.679874837, 0.500000000) B(0.679874897, 0.839937449, 0.500000000) B(0.320125103, 0.160062551, 0.500000000) B(0.000000000, 0.000000000, 0.500000000) P(0.333333343, 0.666666687, 0.500000000) P(0.666666627, 0.333333343, 0.500000000)

**Table S5.** Lattice parameters ( $a$  and  $b$ ) of the B<sub>7</sub>P<sub>2</sub>(Li/Na)<sub>n</sub> at 16 different concentrations (n=1-16), and their percentage of change ( $a\%$  and  $b\%$ ) relative to the pristine lattice parameter ( $a = b = 6.12$  Å) of the B<sub>7</sub>P<sub>2</sub> monolayer.

	$a$ (Å)	$\Delta a$ (%)	$b$ (Å)	$\Delta b$ (%)
B <sub>7</sub> P <sub>2</sub> Li <sub>1</sub>	6.12	0.00%	6.12	0.00%
B <sub>7</sub> P <sub>2</sub> Li <sub>2</sub>	6.11	0.16%	6.13	0.16%
B <sub>7</sub> P <sub>2</sub> Li <sub>3</sub>	6.11	0.16%	6.10	0.33%
B <sub>7</sub> P <sub>2</sub> Li <sub>4</sub>	6.09	0.49%	6.09	0.49%
B <sub>7</sub> P <sub>2</sub> Li <sub>5</sub>	6.13	0.16%	6.13	0.16%
B <sub>7</sub> P <sub>2</sub> Li <sub>6</sub>	6.08	0.65%	6.15	0.49%
B <sub>7</sub> P <sub>2</sub> Li <sub>7</sub>	6.09	0.49%	6.12	0.00%
B <sub>7</sub> P <sub>2</sub> Li <sub>8</sub>	6.10	0.33%	6.10	0.33%
B <sub>7</sub> P <sub>2</sub> Li <sub>9</sub>	6.08	0.65%	6.08	0.65%
B <sub>7</sub> P <sub>2</sub> Li <sub>10</sub>	6.07	0.82%	6.07	0.82%
B <sub>7</sub> P <sub>2</sub> Li <sub>11</sub>	6.05	1.14%	6.05	1.14%
B <sub>7</sub> P <sub>2</sub> Li <sub>12</sub>	6.04	1.31%	6.04	1.31%
B <sub>7</sub> P <sub>2</sub> Li <sub>13</sub>	6.03	1.47%	6.03	1.47%
B <sub>7</sub> P <sub>2</sub> Li <sub>14</sub>	6.01	1.80%	6.01	1.80%
B <sub>7</sub> P <sub>2</sub> Li <sub>15</sub>	6.04	1.31%	6.04	1.31%
B <sub>7</sub> P <sub>2</sub> Li <sub>16</sub>	6.04	1.31%	6.04	1.31%
B <sub>7</sub> P <sub>2</sub> Na <sub>1</sub>	6.13	0.16%	6.13	0.16%
B <sub>7</sub> P <sub>2</sub> Na <sub>2</sub>	6.16	0.65%	6.16	0.65%
B <sub>7</sub> P <sub>2</sub> Na <sub>3</sub>	6.13	0.16%	6.16	0.16%
B <sub>7</sub> P <sub>2</sub> Na <sub>4</sub>	6.15	0.49%	6.16	0.49%
B <sub>7</sub> P <sub>2</sub> Na <sub>5</sub>	6.18	0.98%	6.18	0.98%
B <sub>7</sub> P <sub>2</sub> Na <sub>6</sub>	6.14	0.33%	6.20	1.31%
B <sub>7</sub> P <sub>2</sub> Na <sub>7</sub>	6.18	0.98%	6.18	0.98%

$B_7P_2Na_8$	6.20	1.31%	6.20	1.31%
$B_7P_2Na_9$	6.21	1.47%	6.21	1.47%
$B_7P_2Na_{10}$	6.20	1.31%	6.20	1.31%
$B_7P_2Na_{11}$	6.19	1.14%	6.19	1.14%
$B_7P_2Na_{12}$	6.20	1.31%	6.20	1.31%
$B_7P_2Na_{13}$	6.20	1.31%	6.20	1.31%
$B_7P_2Na_{14}$	6.19	1.14%	6.19	1.14%
$B_7P_2Na_{15}$	6.19	1.14%	6.19	1.14%
$B_7P_2Na_{16}$	6.23	1.80%	6.19	1.14%

**Table S6.** The calculated average adsorption energy ( $E_{ad-ave}$ ) and differential adsorption energy ( $E_{ad-dif}$ ) of Li/Na adsorption on the  $B_7P_2(Li/Na)_n$  with 16 different concentrations

$B_7P_2Li_n$	$E_{ad-ave}-Li(eV)$	$E_{ad-dif}-Li(eV)$	$B_7P_2Na_n$	$E_{ad-ave}-Na(eV)$	$E_{ad-dif}-Na(eV)$
$B_7P_2Li_1$	-1.39	-1.39	$B_7P_2Na_1$	-1.01	-1.01
$B_7P_2Li_2$	-1.03	-0.68	$B_7P_2Na_2$	-0.71	-0.41
$B_7P_2Li_3$	-1.00	-0.93	$B_7P_2Na_3$	-0.57	-0.28
$B_7P_2Li_4$	-1.08	-1.33	$B_7P_2Na_4$	-0.63	-0.80
$B_7P_2Li_5$	-0.98	-0.55	$B_7P_2Na_5$	-0.64	-0.69
$B_7P_2Li_6$	-0.78	+0.19	$B_7P_2Na_6$	-0.55	-0.12
$B_7P_2Li_7$	-0.67	0.00	$B_7P_2Na_7$	-0.50	-0.21
$B_7P_2Li_8$	-0.61	-0.23	$B_7P_2Na_8$	-0.46	-0.16
$B_7P_2Li_9$	-0.54	+0.06	$B_7P_2Na_9$	-0.41	+0.02
$B_7P_2Li_{10}$	-0.51	-0.20	$B_7P_2Na_{10}$	-0.39	-0.22
$B_7P_2Li_{11}$	-0.45	+0.16	$B_7P_2Na_{11}$	-0.36	-0.05
$B_7P_2Li_{12}$	-0.39	+0.25	$B_7P_2Na_{12}$	-0.32	+0.05
$B_7P_2Li_{13}$	-0.35	+0.07	$B_7P_2Na_{13}$	-0.30	-0.08
$B_7P_2Li_{14}$	-0.33	-0.05	$B_7P_2Na_{14}$	-0.30	-0.24
$B_7P_2Li_{15}$	-0.31	+0.02	$B_7P_2Na_{15}$	-0.27	+0.20
$B_7P_2Li_{16}$	-0.28	+0.12	$B_7P_2Na_{16}$	-0.24	+0.13

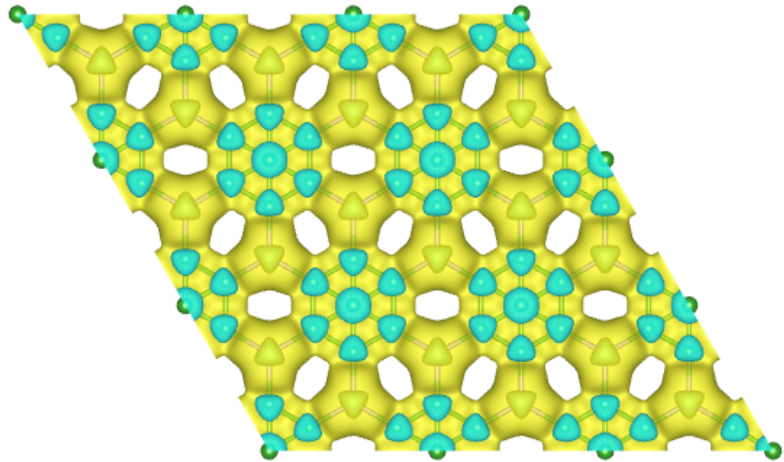


**Fig. S2** Deformation electronic density of the B<sub>7</sub>P<sub>2</sub> monolayer. Light blue and yellow colors denote electron depletion and accumulation regions, respectively. The iso-surface value is 0.005 e/au.

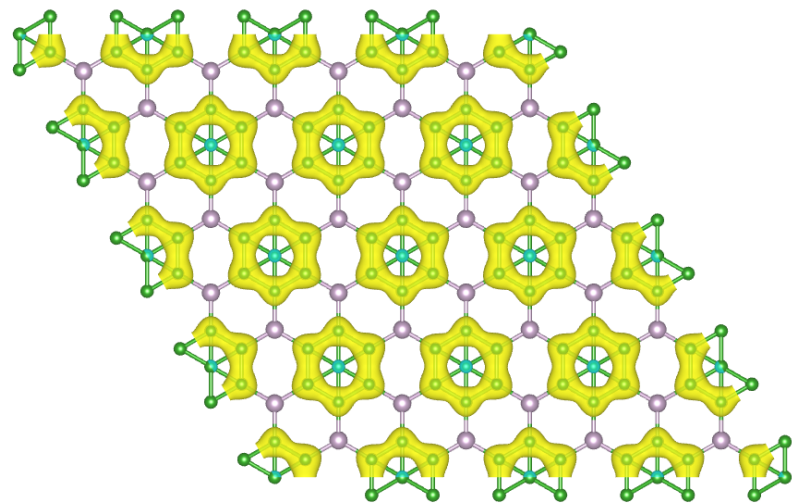


**Fig. S3** Spin density of the ferromagnetic B<sub>7</sub>P<sub>2</sub> monolayer with a value of 0.005 au.

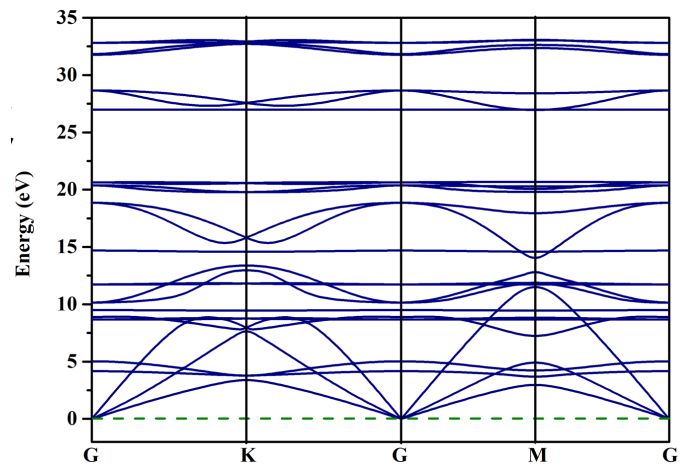


**Fig. S4** Phonon dispersion of the B<sub>7</sub>P<sub>2</sub> monolayer computed using the PBE functional.

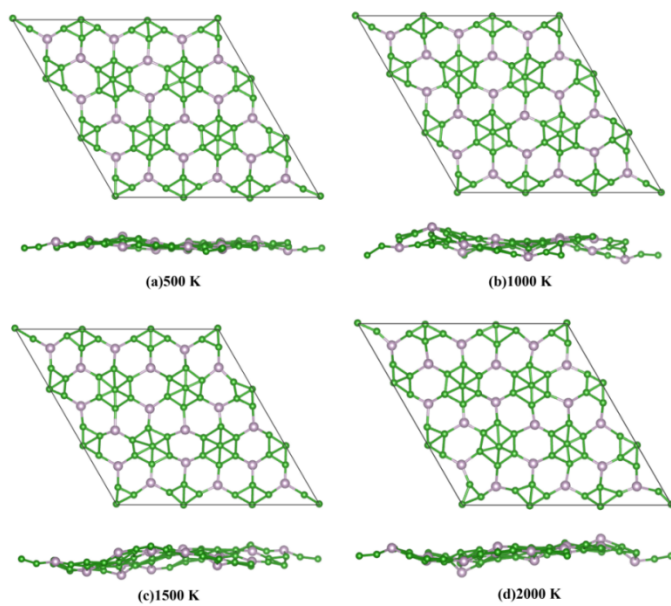


**Fig. S5** Snapshots of the B<sub>7</sub>P<sub>2</sub> monolayer structures at 500 K, 1000 K, 1500 K and 2000 K at the end of 10 ps AIMD simulations.

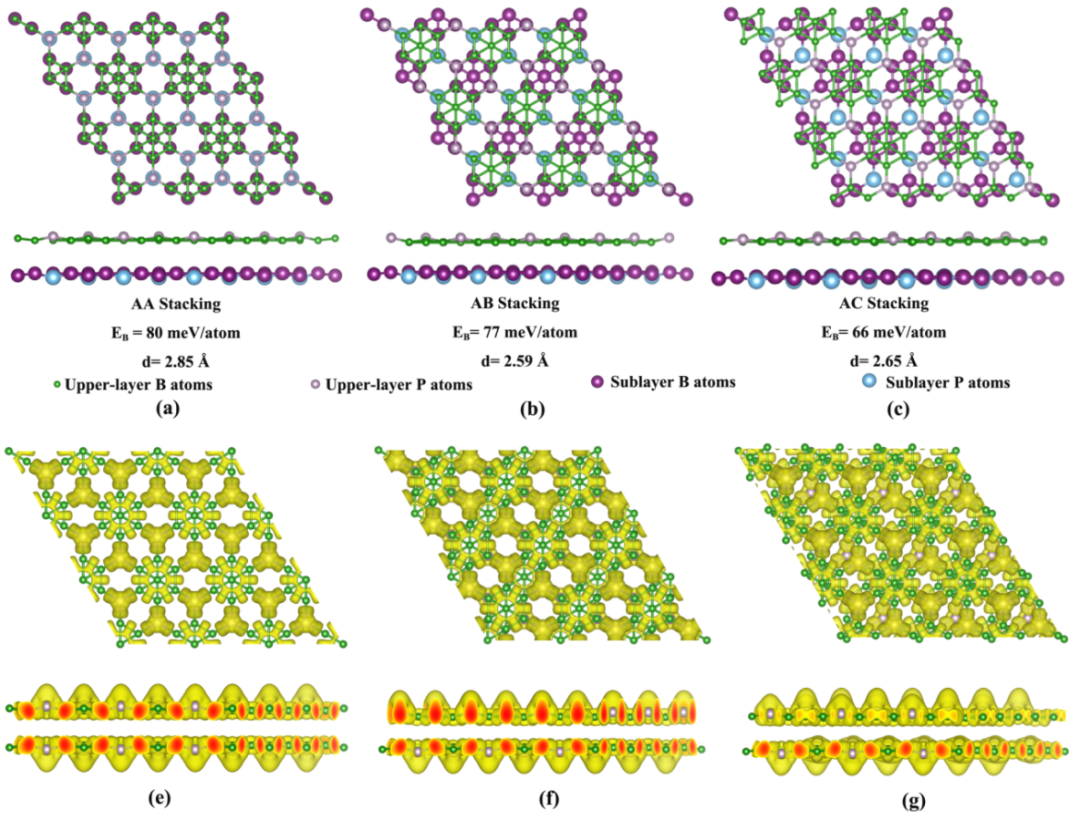


**Fig. S6** (a)-(c) Geometries of the  $\text{B}_7\text{P}_2$  bilayer with AA, AB, and AC stacking patterns.

and their interlayer distances and interaction energies. The interaction energies are defined as  $E_I = (2E_{\text{B}_7\text{P}_2} - E_T)/n$ , in which the  $E_{\text{B}_7\text{P}_2}$  and  $E_T$  are the energies of the  $\text{B}_7\text{P}_2$  monolayer and bilayer,  $n$  is the number of atoms in  $\text{B}_7\text{P}_2$  bilayer. (e)-(f) Isosurface of ELF plotted with a value of 0.50 for the AA, AB and AC stacked bilayers.

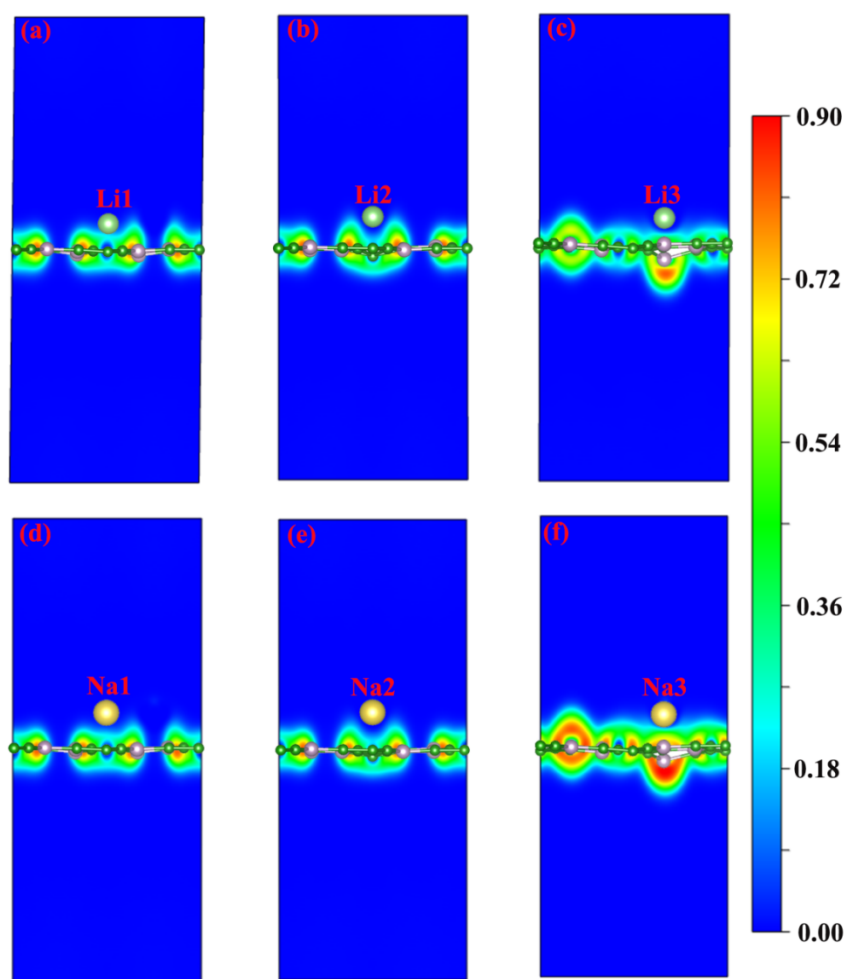


**Fig. S7** ELF map of the B<sub>7</sub>P<sub>2</sub> monolayer adsorbing a single Li/Na atom at three different adsorption sites.

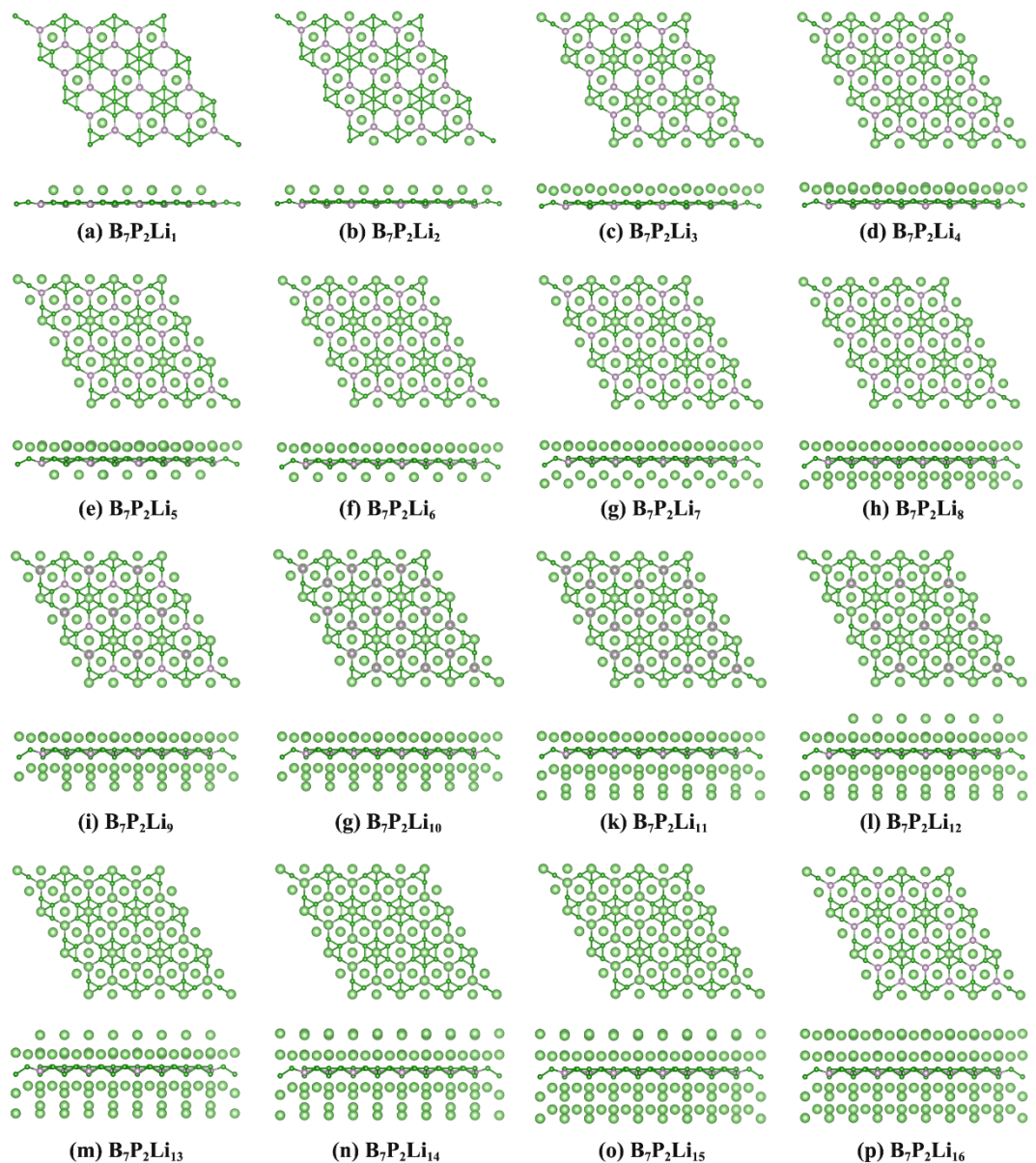


**Fig. S8** The most stable structures of lithiated  $B_7P_2$  monolayer with different Li concentration ( $B_7P_2Li_n$ ,  $n=1-16$ ).

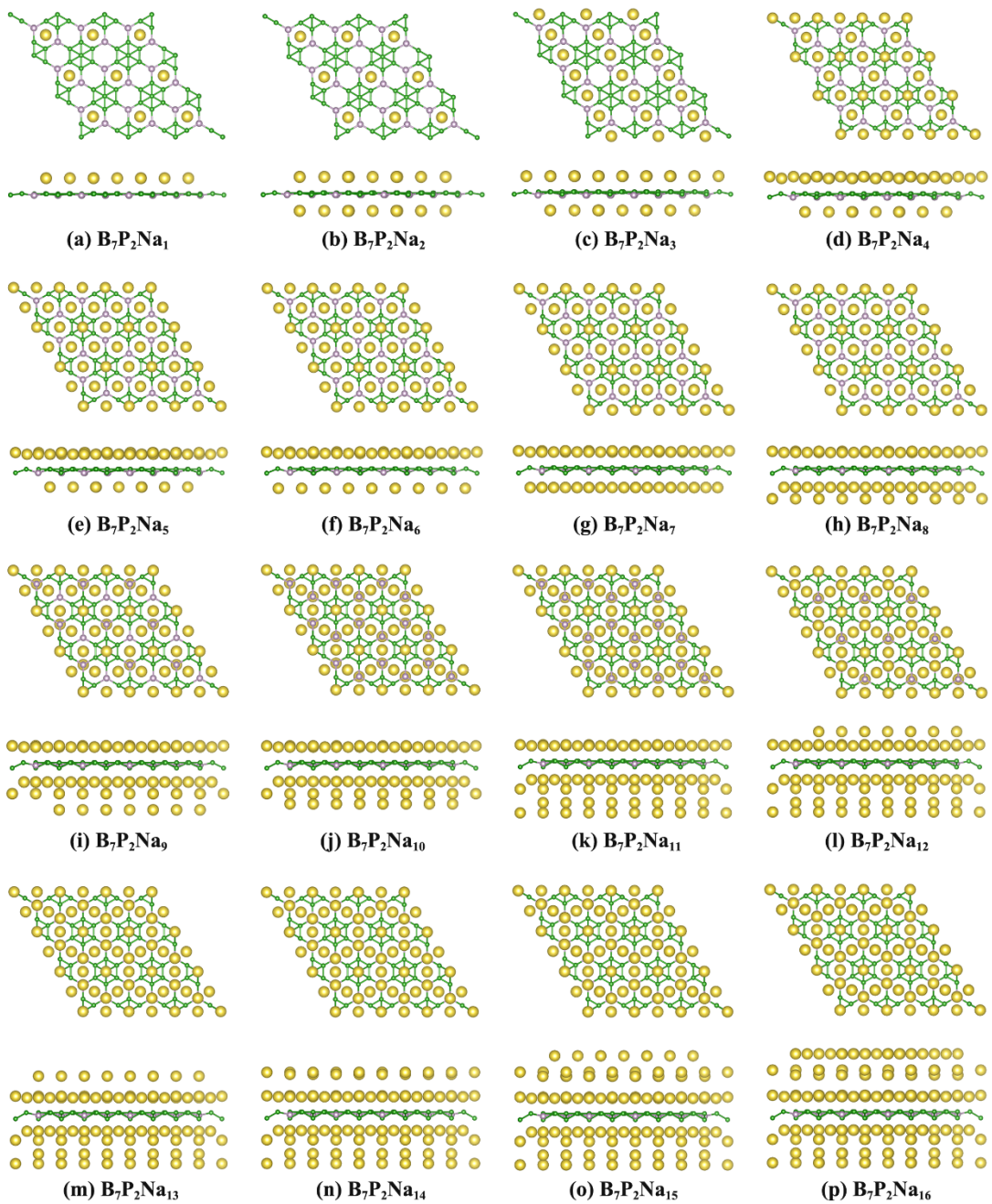


**Fig. S9** The most stable structures of sodiated  $B_7P_2$  monolayer with different Na concentration ( $B_7P_2Na_n$ ,  $n=1-16$ ).

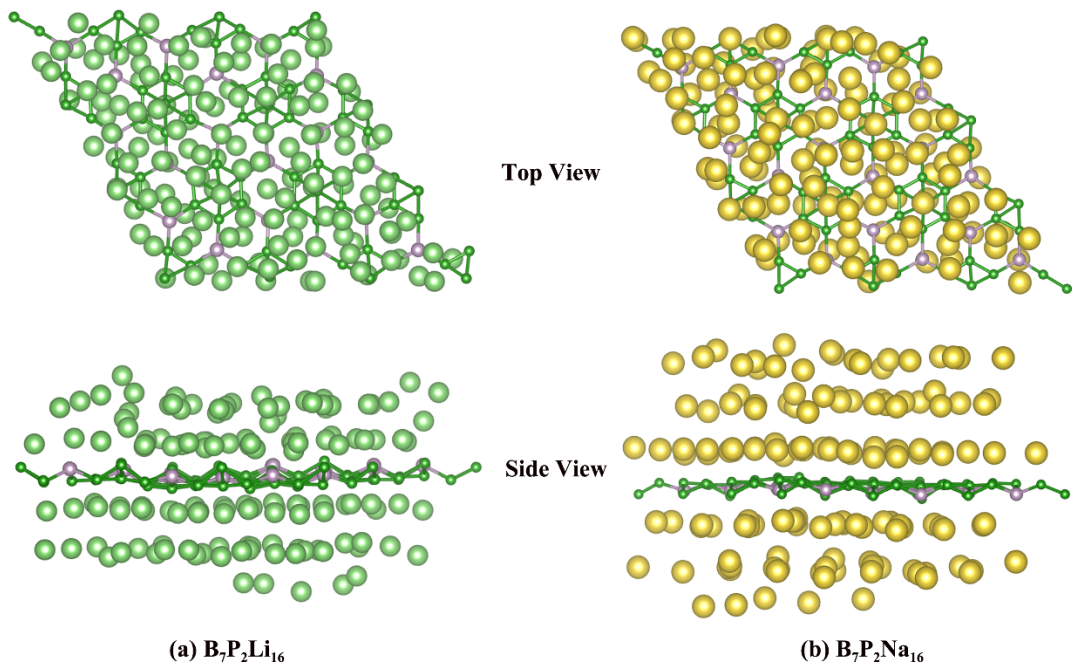


**Fig. S10** Snapshots of (a)  $B_7P_2Li_{16}$  and (b)  $B_7P_2Na_{16}$  structures at 300 K at the end of 10 ps AIMD simulations.

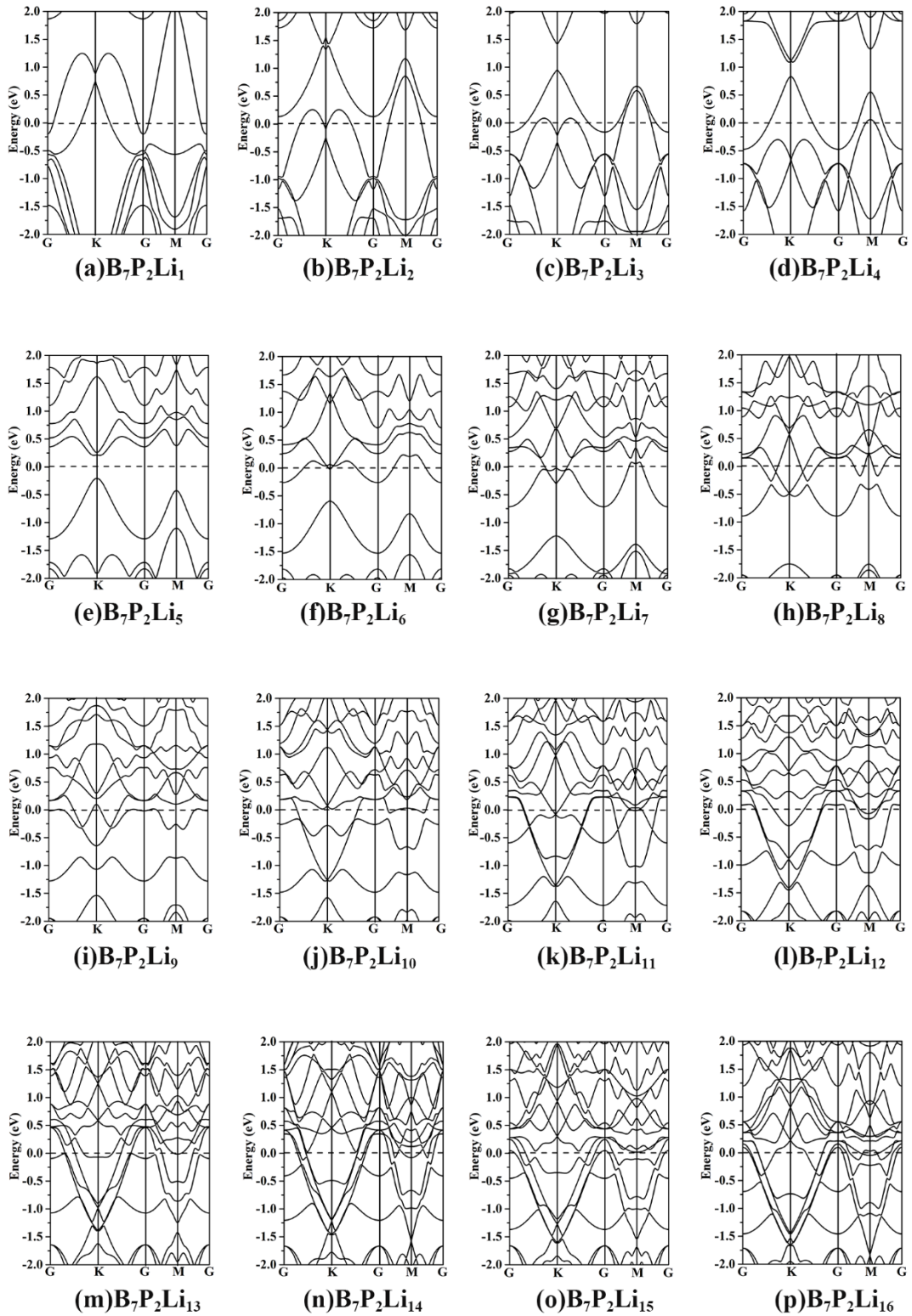


**Fig. S11** Electronic band structure of  $\text{B}_7\text{P}_2\text{Li}_n$  ( $n=1-16$ ) calculated at the PBE level.

The Fermi levels are all set to zero.

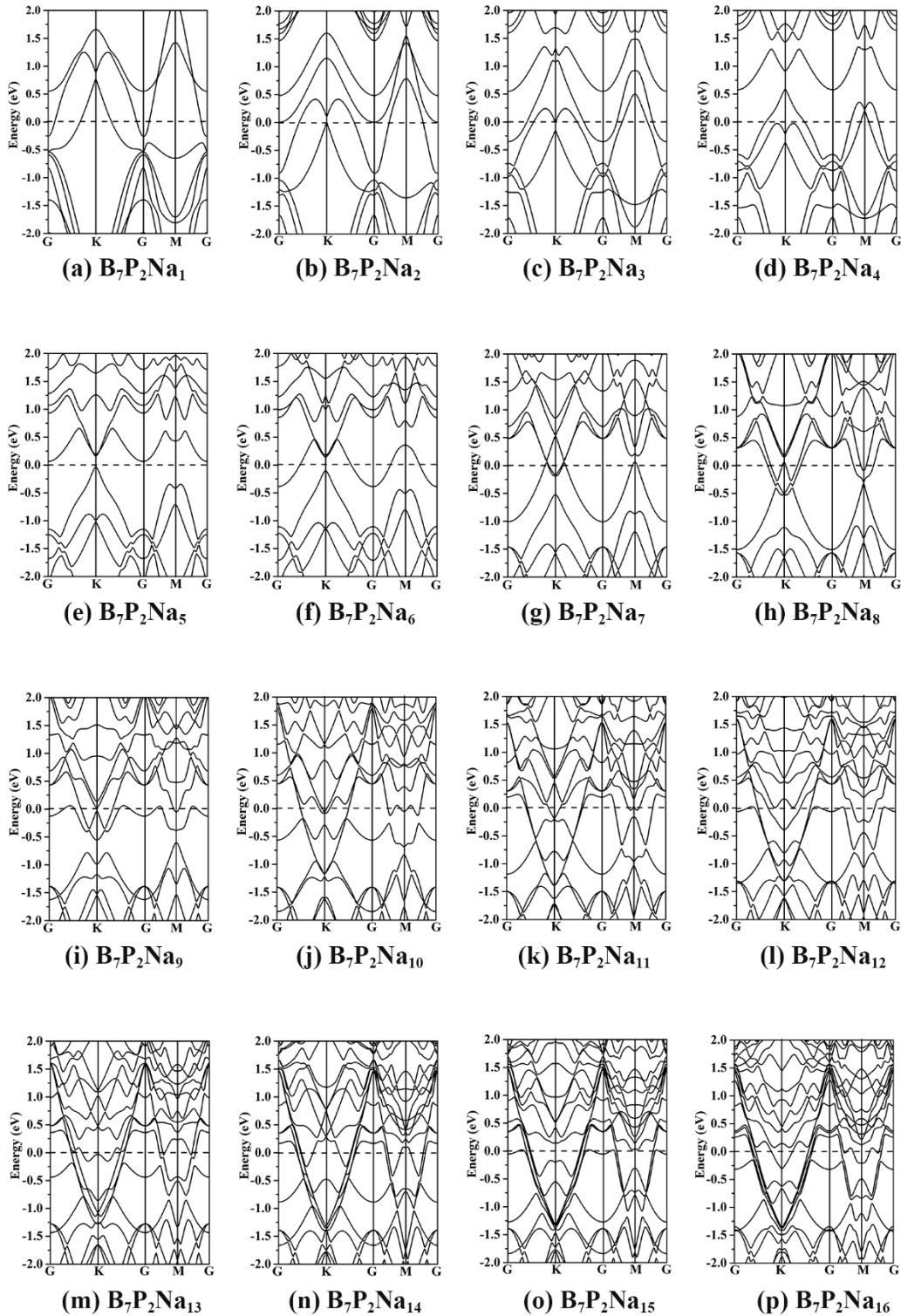


**Fig. S12** Electronic band structure of  $\text{B}_7\text{P}_2\text{Na}_n$  ( $n=1-16$ ) calculated at the PBE level.

The Fermi levels are all set to zero.

## References

- 1 B. Peng, H. Zhang, H. Z. Shao, Y. F. Xu, R. J. Zhang and H. Y. Zhu, *J. Mater. Chem. C*, 2006, **4**, 3592-3598.
- 2 H. Jiang, Z. Lu, M. Wu, F. Ciucci and T. Zhao, *Nano Energy*, 2016, **23**, 97-104.
- 3 D. C. Elias, R. R. Nair, T. M. G. Mohiuddin, S. V. Morozov, P. Blake, M. P. Halsall, A. C. Ferran, D. W. Boukhvalov, M. I. Katsnelson, A. K. Geim and K. S. Novoselov, *Science*, 2009, **323**, 610-613.
- 4 X. Fan, W. Zheng and J. L. Kuo, *ACS Appl. Mater. Interfaces*, 2012, **4**, 2432-2438.
- 5 A. J. Mannix, X. F. Zhou, B. Kiraly, J. D. Wood, D. Alducin, B. D. Myers, X. Liu, B. L. Fisher, U. Santiago and J. R. Guest, *Science*, 2015, **350**, 1513-1516.
- 6 D. B. Putungan, S. H. Lin and J. L. Kuo, *ACS Appl. Mater. Interfaces*, 2016, **8**, 18754-18762.
- 7 X. Zhang, J. Hu, Y. Cheng, H. Y. Yang, Y. Yao and S. A. Yang, *Nanoscale*, 2016, **8**, 15340-15347.